Large Seebeck magnetic anisotropy in thin Co films embedded in Cu determined by *ab initio* investigations

Voicu Popescu* and Peter Kratzer

Faculty of Physics and Center for Nanointegration (CENIDE), University of Duisburg-Essen, Lotharstrasse 1, 47057 Duisburg, Germany

(Received 24 May 2013; revised manuscript received 7 August 2013; published 25 September 2013)

The longitudinal thermopower of a Cu/Co/Cu trilayer system exhibits an oscillatory dependence on the thickness of the Co layer, a behavior related to the formation of quantum well states in the minority spin channel. In addition, it is found to be very sensitive to a switching between an in-plane and out-of-plane magnetization. The resulting magnetothermopower (MTP) is therefore much larger than anticipated from the conventional anisotropic magnetoresistance (AMR). Our calculations establish a direct connection between the magnitude of the MTP signal and the asymmetry of the AMR around the Fermi energy. An enhancement of MTP based on this understanding may offer the possibility of implementing an efficient spin read-out thermoelectric device based on a single ferromagnetic layer.

DOI: 10.1103/PhysRevB.88.104425 PACS number(s): 72.10.−d, 72.15.Jf, 73.50.Jt, 75.30.Gw

I. INTRODUCTION

Exploiting the spin dependence of thermoelectric phenomena triggered the fast development of a new branch in the rich field of spintronics,[1] termed spin caloritronics.[2,3] Recent successful reports on thermally driven spin injection[4] and on detecting a magnetic response of the longitudinal thermopower in multilayered metallic nanowires[5] and tunneling junctions[6] suggested the possibility of a practical magnetothermoelectric device implementation.

The very crux of spintronics is the manipulation and control of the electron spin degree of freedom which, in turn, is coupled to the translational degree of freedom by virtue of the spin-orbit interaction. This ever present phenomenon leads to the occurrence of a magnetization orientation dependence of various materials properties. Its influence on spin-dependent transport ranges from the well-known anisotropic magnetoresistance (AMR)[7,8] to spin-lattice relaxation in metals.[9] The spin-orbit coupling also constitutes the underlying principle of the so-called Dirac logical devices.[10] Here the logical bit is provided through the dependence of electron transmission probability on the relative orientation between the electron spin and the sample magnetization. A typical low/high resistance spin-valve signal upon sweeping an external magnetic field has been demonstrated in tunneling AMR experiments[11,12] employing a *single* ferromagnetic layer, thus offering a major technological advantage over multilayer devices.

The Seebeck effect denotes the appearance of a longitudinal voltage in a sample subjected to a temperature gradient $\vec{\nabla}T$. In a ferromagnetic system this voltage will exhibit a dependence on the angle between the sample magnetization and $\vec{\nabla}T$, a quantity termed magnetothermopower (MTP). In spite of having been measured for various systems,[13–16] the MTP applicability for the practical implementation of a magnetothermoelectric device has not been explored. It is the main purpose of our investigations to show that the MTP may be significantly larger than the AMR and thus could provide an alternative for accomplishing a high-sensitive read-out of a Dirac device. We further investigate the correlation between the MTP and the conventional AMR and find specific conditions for which the former can be maximized.

We consider a Cu/Co$_n$/Cu trilayer system, consisting of an n-monolayer (ML) thick Co slab embedded in Cu(001), as sketched in Fig. 1. While the Co/Cu system is one of the giant magnetoresistance (GMR) prototypes,[17] it is also known to be characterized by a magnetic anisotropy energy (MAE) that oscillates with n.[18,19] This behavior could be related to the appearance of quantum well states (QWSs) in the Co slab. The magnetic anisotropy occurring in this system is caused by the symmetry break-off at the interface and an illustration of its manifestation is provided in Fig. 1(b). The orbital magnetic moments calculated for two different magnetization directions, perpendicular and parallel to the interface, exhibit about 0.005 μ_B difference for the Co interface layers. Remarkably, this interface-localized difference is nearly independent of n.

The setup we propose for detecting a longitudinal MTP signal from a single magnetic layer consists of a thermal gradient taken to be *perpendicular* to the Co/Cu interface, as sketched in Fig. 1(c). We define the MTP as the difference in the calculated Seebeck coefficient for the two magnetization directions, parallel and perpendicular to both temperature and the generated potential gradients. By means of an *ab initio* spin-polarized relativistic approach we account directly, in a parameter free way, for the simultaneous manifestation of spin polarization and spin-orbit coupling.[20] The most important results of our investigations are shown in Fig. 2 and can be summarized as follows: (i) in the range of thin Co slabs, $n \leqslant 6$ ML, the Seebeck coefficient [$S(T)$, top panels] exhibits sign oscillations with n; and (ii) the MTP [$\Delta S(T)$, bottom panels] has large values relative to $S(T)$ over a wide range of temperatures, diminishing at and above $n = 10$ ML. These features are shown to be related to a hybrid band complex formed in the minority spin channel between the QWSs appearing in the Co slab and a high mobility p band present at the Co/Cu interface. The transmission channels provided by these states are more sensitive to the magnetic anisotropy than those derived from bulk states. In addition, their occurrence and energy position is thickness dependent, enabling us to tune the anisotropy effect by varying the thickness of the Co slab.

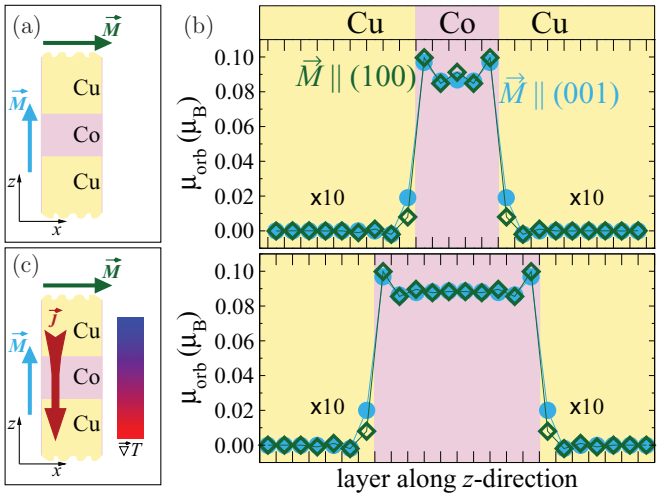

FIG. 1. (Color online) Illustration of spin-orbit coupling induced magnetic anisotropy manifestation in a thin Co slab embedded in Cu(001): (a) Sketch of the geometry of the system, with the two orientations of the magnetization considered here. (b) Orbital magnetization profiles for $\vec{M} \parallel (001)$ (bullets) and $\vec{M} \parallel (100)$ (diamonds) in Co slabs of five (top) and ten (bottom) monolayer (ML) thickness. Note that the orbital magnetic moments of all Cu layers are scaled up by a factor of 10. (c) The setup considered for the longitudinal magnetothermopower, with the current and temperature gradient taken along (001) direction while the magnetization is either parallel or perpendicular to the z axis.

We conclude that whenever a system exhibits in-plane or out-of-plane AMR, a corresponding MTP has to be expected. We find the latter systematically larger; not only is this consistent with the experimental observations,[13,14] but also justified theoretically. Indeed, rather than mapping the Fermi surface alone, the thermoelectric phenomena depend on transmission channels extending over a finite *interval* around the Fermi energy. As a general rule, we find that the MTP is maximized by an enhanced asymmetry in the AMR energy dependence.

II. SYSTEM DESCRIPTION AND THEORETICAL BACKGROUND

Our calculations for the Cu/Co$_n$/Cu trilayer system are performed using a spin-polarized relativistic[20,21] version of the screened Korringa-Kohn-Rostoker Green's function (KKR-GF) method,[22–24] an extremely powerful and versatile scheme that essentially involves two steps. First, the ground state potentials are determined self-consistently for both magnetic configurations $\vec{M} \parallel (001)$ and $\vec{M} \parallel (100)$. In a second step, the self-consistent potentials are used as input for the transport calculation scheme that relies on a relativistic implementation[25] of the Landauer-Büttiker formula within the KKR-GF method.[26,27] The central quantity is represented by the one-electron retarded Green's function $G^+(\vec{r},\vec{r}\,';\varepsilon)$ at energy $\varepsilon = E + i\delta$.

We describe the trilayer system by taking two half-infinite Cu leads with an interaction region inserted in-between, all sharing the same in-plane two-dimensional (2D) periodic lattice. The interaction region contains the n-ML thick Co slab ($n = 3$ to $n = 10$) and up to 10 ML of Cu on both sides of the Co slab. The two half-space potentials are determined from a separate self-consistent calculation and used, through the decimation technique,[28] to provide the boundary conditions for the interaction region potentials. A second self-consistent procedure is applied to the interaction region itself, in which all its potentials are iterated, whereby the outermost Cu potentials asymptotically match the ones of the leads. Since it does not enforce periodic boundary condition along the trilayer growth direction, the advantage of the decimation scheme is twofold: (i) It does not require the additional insertion of separating vacuum layers and (ii) no quantum-well states appear in the leads.

Because of the small lattice misfit between Co and Cu, we neglect the lattice relaxation at the interfaces and take all atomic positions as being fixed to the ideal (001)-stacked fcc lattice with the lattice constant equal to the experimental fcc-Cu value of 3.61 Å. In our calculations we use spherical potentials in the atomic sphere approximation (ASA) determined within the local spin-density approximation.[29] An angular

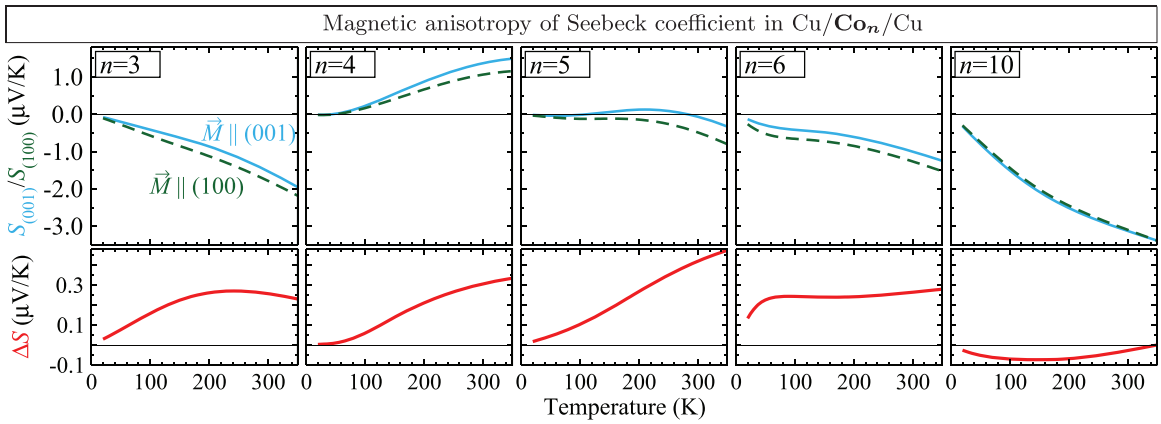

FIG. 2. (Color online) Calculated Seebeck coefficient as a function of temperature T and thickness n ML in the Cu/Co$_n$/Cu trilayer system. Top panels: Seebeck coefficient $S(T)$ determined for two different orientations of the magnetization, parallel [$\vec{M} \parallel (001)$ solid lines] and perpendicular [$\vec{M} \parallel (100)$ dashed lines] to the growth direction, as sketched in Fig. 1(c). Bottom panels: Difference $\Delta S(T) = S_{(001)}(T) - S_{(100)}(T)$ defining the MTP.

momentum cutoff of $l_{\max} = 3$ was taken for the Green's function expansion and $2\,l_{\max} = 6$ for the charge density.

As a consequence of the 2D periodicity of the layered system, the Green's function can be Fourier transformed in a 2D representation with the Bloch vector $\vec{k}_\parallel$ as constant of motion and retaining an index i for the position along the growth direction z. Within the KKR-GF scheme, the Green's function is expressed in terms of the structural Green's function matrix $\underline{G}^{ij}(\vec{k}_\parallel,\varepsilon)$. This matrix describes the propagation of the electron wave between the atomic sites i and j at positions $\vec{R}_i$, $\vec{R}_j$ and is labeled by the relativistic quantum numbers $\Lambda = (\kappa,\mu)$, i.e., $(\underline{A})_{\Lambda\Lambda'} = A_{\Lambda\Lambda'}$.[20] Combined with the matrices $\underline{M}^i$, $\underline{M}^j$ of the z component of the relativistic current operator at sites i and j, it allows one to express the transmission probability between two atomic planes I and J of a 2D system as[25]

$$\mathcal{T}(\vec{k}_\parallel,E) = \sum_{i\in I,\,j\in J} \mathrm{Tr}[\underline{M}^{i\dagger}\underline{G}^{ij}(\vec{k}_\parallel,\varepsilon)\underline{M}^{j}\underline{G}^{ij\dagger}(\vec{k}_\parallel,\varepsilon)], \quad (1)$$

where each 2D vector $\vec{k}_\parallel$ can be seen as a conduction channel.[27] An integration over the 2D Brillouin zone (2D-BZ) provides the total transmission probability $\mathcal{T}(E)$ at energy E[27]:

$$\mathcal{T}(E) = \frac{1}{A_{\text{2D-BZ}}} \int_{\text{2D-BZ}} d^2\vec{k}_\parallel \mathcal{T}(\vec{k}_\parallel,E). \quad (2)$$

The energy-dependent transmission given in Eq. (2) is used to determine the transport coefficients[30]:

$$L^{(\alpha)}(T) = -\int (\partial_E f_0)\mathcal{T}(E)\,(E-\mu)^\alpha\, dE, \quad (3)$$

where $f_0 \equiv f_0(E,T,\mu)$ is the Fermi-Dirac distribution function at energy E, temperature T, and chemical potential μ, with $\partial_E f_0 = \partial f_0/\partial E$ its energy derivative. Knowledge of these quantities allows one to calculate the Seebeck coefficient $S(T)$ as

$$S(T) = -\frac{1}{eT}\frac{L^{(1)}}{L^{(0)}}, \quad (4)$$

where the denominator is related to the temperature dependent conductance $g(T)$ by

$$g(T) = \frac{e^2}{h}L^{(0)}. \quad (5)$$

We should mention here that the dependence of the self-consistent potentials and the transport properties on the magnetization direction is implicitly taken into account by solving the Dirac equation in the local frame of reference at each atomic site. Unitary rotations are afterwards applied to obtain the Green's function in the global frame of reference with the quantization axis parallel to the z axis.[20]

The formalism described above only considers elastic scattering of the electrons by the interfaces, whereas inelastic scattering processes, such as scattering by phonons or spin fluctuations, are neglected. At elevated temperatures, these scattering mechanisms will certainly play a role, in particular for the temperature dependence of the conductivity. It has been demonstrated, for example, that inclusion of electron scattering by spin fluctuations in various ferromagnetic metals and alloys leads to a better agreement of the temperature dependent resistivity with experimental data.[31,32] Since these effects become important when approaching the Curie temperature, we restrict our investigations to a temperature range below 350 K. We note in addition that $S(T)$ being the quotient of $L^{(1)}(T)$ and $L^{(0)}(T)$, any additional temperature dependence due to inelastic scattering, appearing both in the numerator and the denominator, tends to cancel out, as long as phonon drag effects can be disregarded. In view of these factors, we consider our treatment of the Seebeck coefficient quite reliable in the temperature range considered.

III. MAGNETOTHERMOPOWER RESULTS AND THEIR INTERPRETATION

The electronic structure and transport properties of Co/Cu systems have been intensively studied.[33–37] It is now common knowledge that their majority spin d band is almost completely full and the energy range at and near the Fermi level is dominated by the $3d$ minority states stemming from Co. Two important consequences arise as a result of these characteristics of the electronic structure: (i) Significant quantitative and qualitative differences are present in the transmission through the two spin channels; and (ii) minority spin quantum well states (QWSs) appear in the Co layer. The latter have been identified to be responsible for the oscillatory behavior of the magnetic anisotropy energy (MAE),[38] that was evidenced both experimentally[18] and theoretically[19] in the Cu/Co$_n$/Cu trilayers.

Both of these features could be reproduced by our calculations. First, a spin decomposition of $\mathcal{T}(E)$, performed as prescribed in Ref. 25, has shown significant differences between the two spin channels. While the majority spin transmission $\mathcal{T}^{\text{maj}}(E)$ has a smooth, featureless energy dependence, the minority spin $\mathcal{T}^{\text{min}}(E)$ is reduced in strength by about a factor of 2 and exhibits a significant nonmonotonous behavior. Second, we could determine signatures of QWSs by performing an angular momentum and $\vec{k}_\parallel$ decomposition of the local density of states. We begin our discussion by focusing on these particular states. It will be shown that they provide efficient transmission channels at energy positions that are thickness dependent and sensitive to the magnetic anisotropy in the system. Our findings for the Seebeck coefficient and the MTP will then be linked to these peculiarities of the electronic structure.

A. Quantum well states in the Co slab

The minority spin channel QWSs appearing in the Co slab have been investigated by calculating the angular momentum and atom projected Bloch spectral function $A(\vec{k}_\parallel,E)$,[20] a quantity that can be regarded as a $\vec{k}_\parallel$-resolved density of states (DOS). Figure 3 depicts the minority spin component of $A(\vec{k}_\parallel,E)$ projected on the first Co layer near the Cu/Co interface for various values of the Co thickness n and for $\vec{M} \parallel (001)$ configuration. Such E versus $\vec{k}_\parallel$-type plots allow us to identify the projected band structure in the 2D-BZ, a picture familiar from angle-resolved photoemission experiments.

The very appearance of the QWSs will depend on n, alternating between odd and even number of ML. For a given parity, on the other hand, the n dependence is reflected in a variation in the energy position of the QWSs. Typical

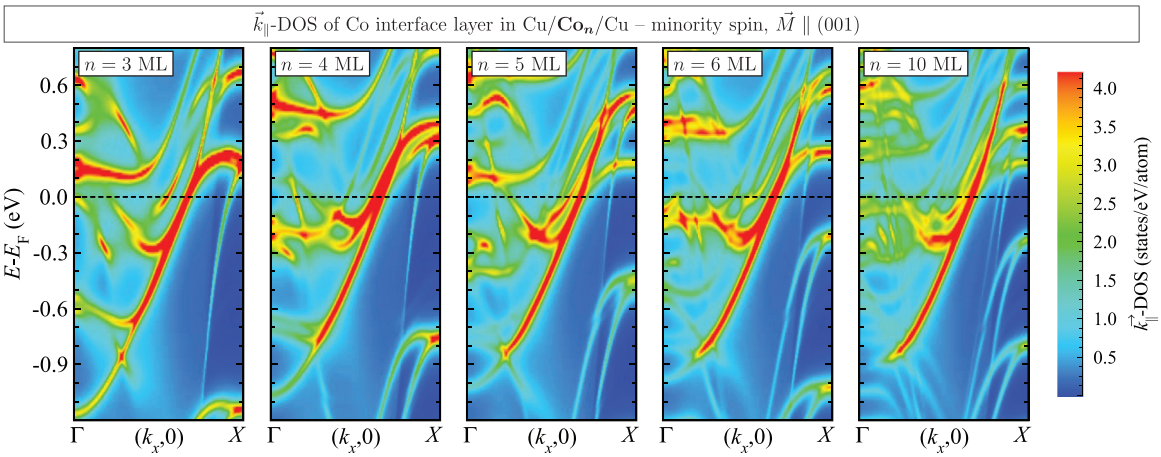

FIG. 3. (Color online) Minority spin $\vec{k}_\parallel$-resolved DOS projected on the interface Co layer in the Cu/Co$_n$/Cu trilayer system for various values of n with $\vec{M} \parallel (001)$. A p-type band crossing the Fermi energy (taken here as reference value) is evidenced, as well as typical signatures of QWSs appearing as flat bands above (odd n) and below (even n) E_F for thin Co slabs.

signatures of QWSs can be observed as flat bands near the 2D-BZ center: (i) around 0.15 eV for $n = 3$ and $n = 5$ and (ii) around -0.2 eV and 0.45 eV for $n = 4$ and $n = 6$, all values relative to the Fermi energy. With increased thickness of the Co slab, the QWSs morph into a continuum, as seen in the rightmost panel of Fig. 3.

Even more important, however, is the finding that the QWSs couple with the high-mobility minority spin p band that crosses the Fermi energy. This band, evidenced by the enhanced S-shaped feature (red/dark gray) of the spectral function in Fig. 3, stems from the Cu and Co atoms adjacent to the interface and shows no thickness dependence. As a result of this coupling, a p-d hybrid complex is formed which will be shown in the following to provide efficient transmission channels. As the appearance of this complex in a particular energy window is thickness dependent, it is obvious that the associated transmission can be "turned on or off" by changing n. Furthermore, because of their character, combining high-mobility p and QWS d-like states, these channels are most affected by the magnetic anisotropy. While here we show $A(\vec{k}_\parallel, E)$ only for $\vec{M} \parallel (001)$, subtle changes appear in these states upon flipping the magnetization, accordingly reflected in the transmission probability.

B. Anisotropic magnetoresistance in Cu/Co/Cu trilayers

We have shown in Fig. 1(b) that the orbital magnetic moments in Cu/Co$_n$/Cu change upon flipping the magnetization direction, in particular on the Co and Cu atoms close to the interfaces. The spin-orbit coupling further leads to an anisotropic transmission probability, as shown in Fig. 4 for a Co slab thickness of 4 ML. Here we make a side-by-side comparison of the $\vec{k}_\parallel$-resolved transmission $\mathcal{T}(\vec{k}_\parallel, E)$ for $\vec{M} \parallel (001)$ (left panel) and $\vec{M} \parallel (100)$ (right panel). In all our calculations we used a 1000×1000 regular grid in the full 2D-BZ and the transmission is shown here for an argument $E = E_F - 0.16$ eV. This corresponds to the maximum in the minority spin interface Co spectral function associated with the QWS-p complex shown in Fig. 3 for $n = 4$ ML.

The magnetic anisotropy in transmission is reflected both qualitatively and quantitatively: While $\mathcal{T}_{(001)}(\vec{k}_\parallel, E)$ has a fourfold, $\mathcal{T}_{(100)}(\vec{k}_\parallel, E)$ only has a twofold rotation symmetry. In addition, a clear reduction occurs in transmission for $\vec{M} \parallel (100)$, for example in the vicinity of the zone center (at normal incidence) and in the pronounced, petal-shaped features extending along the k_x and k_y axes. These strong transmission channels can be identified to be precisely those related to the minority spin p-d hybrid states originating from the coupling of the interface Co/Cu p band and the QWSs.

The importance of this minority spin p-d complex becomes more clear by inspecting the transmission probability $\mathcal{T}(E)$ integrated over all $\vec{k}_\parallel$ transmission channels, shown for several values of n in Fig. 5. One can easily follow the evolution of the two major peaks in $\mathcal{T}_{(100)}(E)$ and $\mathcal{T}_{(001)}(E)$ located around -0.6 and -0.16 eV below E_F for $n = 4$, shifted upwards for $n = 6$, and no longer present for $n = 10$, actually tracking the evolution of the QWS-related p-d complex and illustrating the anticipated on-off behavior obtained through the thickness variation. These changes in the transmission probability profile

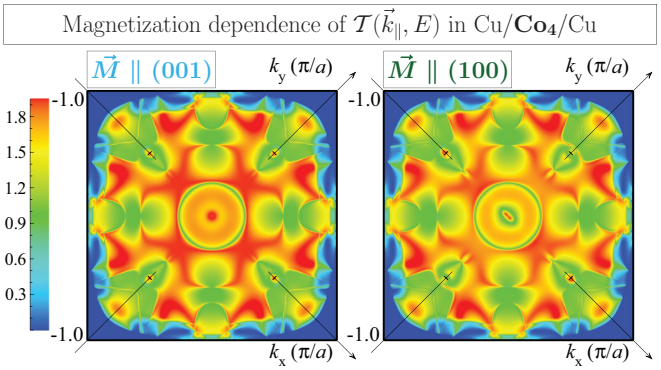

FIG. 4. (Color online) Comparison of the $\vec{k}_\parallel$-resolved transmission $\mathcal{T}(\vec{k}_\parallel, E)$ in the Cu/Co$_4$/Cu trilayer system for $\vec{M} \parallel (001)$ (left) and $\vec{M} \parallel (100)$ (right). The plot area comprises the full 2D-BZ and the energy argument is $E = E_F - 0.16$ eV.

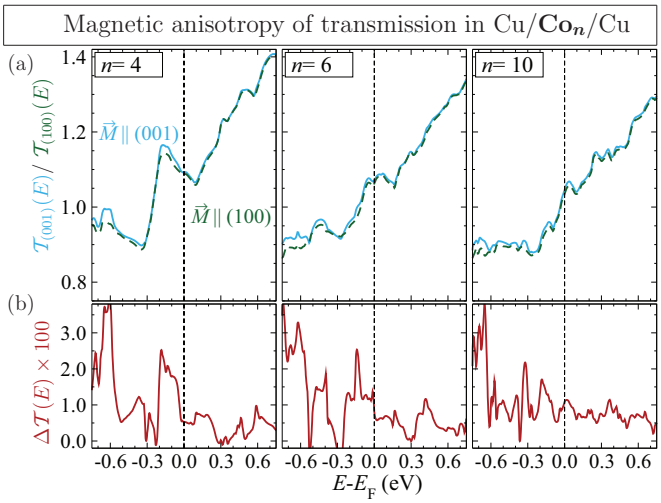

FIG. 5. (Color online) Dependence of transmission probability on Co thickness and magnetization direction in the Cu/Co$_n$/Cu trilayer system for $n = 4$, 6, and 10 (from left to right). (a) Energy-dependent transmission $\mathcal{T}(E)$ [Eq. (2)] shown here for both orientations of the magnetization, $\vec{M} \parallel (001)$ (solid line) and $\vec{M} \parallel (100)$ (dashed line); and (b) difference in transmission $\Delta\mathcal{T}(E) = \mathcal{T}_{(001)}(E) - \mathcal{T}_{(100)}(E)$. A scale factor of 100 has been applied to $\Delta\mathcal{T}(E)$.

have a significant impact on the electronic contribution to the Seebeck coefficient calculated via Eq. (4).

In the bottom panels of Fig. 5 we show the transmission difference $\Delta\mathcal{T}(E) = \mathcal{T}_{(001)}(E) - \mathcal{T}_{(100)}(E)$, which can be seen as a measure of the energy-dependent AMR. Plotting $\Delta\mathcal{T}(E)$ rather than the AMR ratio $(g_{(001)} - g_{(100)})/g_{(100)}$ enables us a more direct comparison with $\Delta S(T)$. We note that, by virtue of Eq. (5), $g(E) = (e^2/h)\mathcal{T}(E)$ in the limit of $T \to 0$.

It can be seen from Fig. 5(b) that $\Delta\mathcal{T}(E)$ is quite small. From its relative magnitude to $\mathcal{T}_{(100)}(E)$ one can estimate an overall AMR not exceeding 2%. Notable exceptions are few energy intervals, e.g., immediately below E_F for $n = 4$ and $n = 6$, characterized by AMR values as high as 5%. These maxima in $\Delta\mathcal{T}(E)$ coincide exactly with the energy location of the QWS-p-band complexes. The overall small value of the AMR is in stark contrast with the calculated MTP, where relative changes of up to 90% could be determined for thin Co slabs. As will be shown in the following, the large MTP is a direct consequence of this particular energy dependence of $\Delta\mathcal{T}(E)$ in the immediate vicinity of E_F.

C. Magnetothermopower versus AMR

The knowledge gained so far on the n dependence of the transmission probability allows a straightforward interpretation of our results for the Seebeck coefficient and the MTP presented in Fig. 2. Both are directly related to $\mathcal{T}(E)$, the central quantity in our approach, through Eq. (4). This expression essentially contains the two transport coefficients: $L^{(0)}$ in the denominator and $L^{(1)}$ in the numerator, determined according to Eq. (3) with $\alpha = 0$ and $\alpha = 1$, respectively. The former also provides the temperature dependent conductance $g(T)$ given by Eq. (5). We note that a temperature increase, in the present formalism, is equivalent to an actual extension of the energy integration window in Eq. (3).

While the denominator of Eq. (4) only influences the size of $S(T)$, the numerator will determine both its size *and* its sign. Thus, a dominant transmission above (below) the Fermi energy will result in a negative (positive) Seebeck coefficient, a well established method to determine the type of conductivity, n or p, in doped semiconductors.

As pointed out by Czerner *et al.*[39] the numerator of Eq. (4) may be seen as a "center of mass" of $\mathcal{T}(E)\partial_E f_0(E,T,\mu)$. From this analogy it is obvious that the sign and value of $L^{(1)}$, correspondingly reflected in $S(T)$, is extremely sensitive to small changes in its integrand below or above E_F caused by an increased temperature. It furthermore shows that one of the paths towards maximizing the Seebeck coefficient is to enhance the asymmetry of transmission around the Fermi level, since the skewness term $(E - E_F)$ occurring in $L^{(1)}$ is an antisymmetric function about E_F.

As seen in Fig. 2, the Seebeck coefficient $S(T)$ for $n \leqslant 6$ ML is small, not exceeding an absolute value of few μV/K. In addition, it exhibits an alternating sign, almost independent of the magnetization orientation: $S(T)$ is negative for $n \leqslant 3$ and $n \geqslant 6$ ML, but gets positive for $n = 4$. The 5 ML thick Co slab stands out through its very small valued $S(T)$.

This evolution of the Seebeck coefficient with the Co thickness n and the electronic temperature T is intimately connected with the energy dependence of the transmission and with the presence of the QWS-p hybrid complex discussed above. As shown in Fig. 3, while these states are indeed at ± 0.15 eV relative to the Fermi energy, they have tails extending and actually crossing E_F. These features are accordingly reflected in the $\mathcal{T}(E)$ curves, for example by the wide shoulder below E_F for $n = 4$, leading to the positive $S(T)$ at this thickness. The fluctuations in the QWSs energy positioning, above and below the Fermi energy for odd and even n induce in this way the sign oscillations in $S(T)$, an analogous behavior to that observed for the MAE.

As the thickness of the Co slab increases, the relative contribution related with the Co/Cu interfaces diminishes. The transmission is enhanced above the Fermi energy as a result of an increased s- and p-DOS, states characterized by a high mobility. For larger n values, $S(T)$ begins to take on negative values, typical for the late transition metals. We should note at this point that *ab initio* calculations using the Kubo-Greenwood formalism[40] predicted for bulk Co a Seebeck coefficient ranging between $\simeq -3$ μV/K at 100 K and $\simeq -11$ μV/K at 500 K in fairly good agreement with the experimental data.[40] Measurements on Ni and Fe-Ni films,[16] on the other hand, have shown that even at a 20 nm thickness of the sample, the Seebeck coefficient is about half the value measured for bulk.

While the top panels of Fig. 2 show $S_{(001)}(T)$ and $S_{(100)}(T)$ calculated for different orientations of the magnetization [$\vec{M} \parallel (001)$ and $\vec{M} \parallel (100)$], the bottom panels depict the difference between the two configurations $\Delta S(T) = S_{(001)}(T) - S_{(100)}(T)$. We use this quantity for plotting purposes rather than the relative difference $\Delta S(T)/\min\{|S_{(001)}(T)|, |S_{(100)}(T)|\}$ to avoid discontinuities caused by the sign change in its denominator. It can easily be seen that $\Delta S(T)$ is positive for $n < 10$ and relatively large, comparable in size with $S(T)$ for $n = 4$–6 ML. At this thickness, one can estimate the relative difference to be about 90% at low temperatures, steadily

decreasing to a value of $\simeq$25% for $n = 6$ at room temperature. As n increases to 10 ML and above, $\Delta S(T)$ drops to few percent of $S(T)$, comparable with the 6% value measured for GaMnAs films.[13]

These large values for the MTP are in strong contrast with those of the conventional AMR discussed above and shown in Fig. 5(b). Indeed, we found an ubiquitous spin-orbit coupling induced magnetic anisotropy in $\mathcal{T}(E)$, but with very small values, except for maxima in the energy regions of the QWSs. Once the sharp QWSs render into a continuum with increasing n these maxima start to disappear. Comparison of $\Delta\mathcal{T}(E)$ in Fig. 5 with $\Delta S(T)$ in Fig. 2 reveals two important facts: (i) The MTP can be relatively large without requiring a correspondingly large AMR; and (ii) $\Delta S(T)$ drops significantly, by a factor of 3 in absolute value, at large n values.

It is important to realize that this severe drop in the MTP is not following a dramatic change in the overall values of the AMR at different energies but rather in their distribution. With increasing Co thickness n, the asymmetry of $\Delta\mathcal{T}(E)$ in the immediate vicinity of E_F is reduced. This relation between the energy dependence of $\Delta\mathcal{T}(E)$ and the size of $\Delta S(T)$ can again be understood on the basis of Eq. (4). Taking the denominators for the two magnetic configurations approximately equal, $g_{(001)}(T) \simeq g_{(100)}(T)$, it follows that, to leading order:

$$\Delta S(T) \simeq \int dE(\partial_E f_0)(E - E_F)\,\Delta\mathcal{T}(E), \qquad (6)$$

and thus, since $(E - E_F)$ is antisymmetric about E_F, a $\Delta\mathcal{T}(E)$ of odd parity about E_F is needed to maximize the MTP, $\Delta S(T)$. We emphasize here on the analogy with the condition for $S(T)$, which is maximized by an asymmetry of $\mathcal{T}(E)$.

In the materials system studied here, Cu/Co$_n$/Cu, where the magnetic anisotropy manifests itself mostly via the QWSs, E_F is typically located on a rising or falling flank of a transmission resonance due to the QWSs. Due to the sensitivity of the Seebeck coefficient on the slope of $\mathcal{T}(E)$, the MTP is a more sensitive probe than the AMR in systems of this type.

Finally, a comment on the possible effect of the lattice vibrations on our results is in order. We note that, at the temperatures considered, the thickness of the Co slabs is smaller than the mean free path for electron-phonon scattering, and hence inelastic scattering of the electrons within the Co layer is unlikely. However, the coupling to lattice vibrations will broaden the QWSs and thus tend to wash out the structure in $\Delta\mathcal{T}(E)$, which would diminish the MTP. The temperature scale for this to happen is set by the energy spacing between QWSs compared to typical thermal energies of $k_B T$.

IV. CONCLUSIONS

We have shown by *ab initio* calculations that a large longitudinal magnetothermopower (MTP) can appear in ferromagnetic Cu/Co$_n$/Cu systems under a thermal gradient parallel with the growth direction, in spite of a small anisotropic magnetoresistance (AMR). The calculated Seebeck coefficient exhibits, in the range of thin Co slabs, an oscillatory dependence on n, a behavior that, analogous to the oscillations in the magnetic anisotropy energy, could be linked with the quantum well states (QWSs) appearing in the Co spacer. We have found that increasing the thickness of the Co slab beyond 10 ML causes the MTP to diminish, which correlated with a more symmetric distribution of the AMR in the vicinity of the Fermi energy rather than with its reduction in amplitude.

In the present system, the occurrence of QWSs allowed us to tune the asymmetry of $\Delta\mathcal{T}(E)$ by changing the number of Co monolayers. To make use of this possibility, atomically sharp and smooth interfaces are required that lead to well defined QWSs. However, we note that the occurrence of a large longitudinal MTP is more general and applies to a wider class of magnetic materials. In systems with a crystal structure lacking inversion symmetry and/or containing heavy elements, the AMR, and hence the MTP, are less interface dependent. We therefore expect that a large MTP can be observed in such systems with lower demands on the structural perfection of the interfaces.

We suggest that, analogously to the tunneling AMR in electronic conductance, the MTP could provide a spin-valve signal and thus be used in a magnetothermoelectric logical device. While any system with a finite AMR will always exhibit an MTP, we emphasize the fact that the relative magnitude between the two effects will depend on the degree of asymmetry in the energy dependence of the former. As such, enhancing the AMR asymmetry about the Fermi energy provides a direct path to increase the MTP and so to maximize the signal resolution.

ACKNOWLEDGMENTS

This work was supported by the German Research Foundation (*Deutsche Forschungsgemeinschaft—DFG*) within the Priority Program 1538 "Spin Caloric Transport (SpinCaT)." The authors gratefully acknowledge the computing time granted by the John von Neumann Institute for Computing (NIC) and provided on the supercomputer JUROPA at Jülich Supercomputing Centre (JSC). Additional computer facilities have been offered by the Center for Computational Sciences and Simulation (CCSS) at the University Duisburg-Essen.

*voicu.popescu@uni-due.de

[1] E. Y. Tsymbal and I. Žutić (eds.), *Handbook of Spin Transport and Magnetism* (Chapman and Hall/CRC, Boca Raton, FL, 2011).

[2] G. E. W. Bauer, E. Saitoh, and B. J. van Wees, Nat. Mater. **11**, 391 (2012).

[3] B. Scharf, A. Matos-Abiague, I. Žutić, and J. Fabian, Phys. Rev. B **85**, 085208 (2012).

[4] A. Slachter, F. L. Bakker, J. P. Adam, and B. J. van Wees, Nat. Phys. **6**, 879 (2010).

[5] L. Gravier, S. Serrano-Guisan, F. Reuse, and J.-P. Ansermet, Phys. Rev. B **73**, 024419 (2006).

[6] M. Walter, J. Walowski, V. Zbarsky, M. Münzenberg, M. Schäfers, D. Ebke, G. Reiss, A. Thomas, P. Peretzki, M. Seibt *et al.*, Nat. Mater. **10**, 742 (2011).

[7]J. Smit, Physica **17**, 612 (1951).
[8]I. A. Campbell, A. Fert, and O. Jaoul, J. Phys. C **3**, S95 (1970).
[9]B. Zimmermann, P. Mavropoulos, S. Heers, N. H. Long, S. Blügel, and Y. Mokrousov, Phys. Rev. Lett. **109**, 236603 (2012).
[10]J. Sinova and I. Žutić, Nat. Mater. **11**, 368 (2012).
[11]C. Gould, C. Rüster, T. Jungwirth, E. Girgis, G. M. Schott, R. Giraud, K. Brunner, G. Schmidt, and L. W. Molenkamp, Phys. Rev. Lett. **93**, 117203 (2004).
[12]C. Ruster, C. Gould, T. Jungwirth, E. Girgis, G. M. Schott, R. Giraud, K. Brunner, G. Schmidt, and L. W. Molenkamp, J. Appl. Phys. **97**, 10C506 (2005).
[13]Y. Pu, E. Johnston-Halperin, D. D. Awschalom, and J. Shi, Phys. Rev. Lett. **97**, 036601 (2006).
[14]P. Wiśniewski, Appl. Phys. Lett. **90**, 192106 (2007).
[15]A. D. Avery, M. R. Pufall, and B. L. Zink, Phys. Rev. Lett. **109**, 196602 (2012).
[16]A. D. Avery, M. R. Pufall, and B. L. Zink, Phys. Rev. B **86**, 184408 (2012).
[17]M. A. M. Gijs and G. E. W. Bauer, Adv. Phys. **46**, 285 (1997).
[18]W. Weber, A. Bischof, R. Allenspach, C. Würsch, C. H. Back, and D. Pescia, Phys. Rev. Lett. **76**, 3424 (1996).
[19]L. Szunyogh, B. Újfalussy, C. Blaas, U. Pustogowa, C. Sommers, and P. Weinberger, Phys. Rev. B **56**, 14036 (1997).
[20]H. Ebert, D. Ködderitzsch, and J. Minár, Rep. Prog. Phys. **74**, 096501 (2011).
[21]H. Ebert *et al.*, *The Munich SPR-TB-KKR Package*, http://www.ebert.cup.uni-muenchen.de/spr-tb-kkr.
[22]L. Szunyogh, B. Újfalussy, P. Weinberger, and J. Kollár, Phys. Rev. B **49**, 2721 (1994).
[23]R. Zeller, P. H. Dederichs, B. Újfalussy, L. Szunyogh, and P. Weinberger, Phys. Rev. B **52**, 8807 (1995).
[24]K. Wildberger, R. Zeller, and P. H. Dederichs, Phys. Rev. B **55**, 10074 (1997).
[25]V. Popescu, H. Ebert, N. Papanikolaou, R. Zeller, and P. H. Dederichs, Phys. Rev. B **72**, 184427 (2005).
[26]H. U. Baranger and A. D. Stone, Phys. Rev. B **40**, 8169 (1989).
[27]P. Mavropoulos, N. Papanikolaou, and P. H. Dederichs, Phys. Rev. B **69**, 125104 (2004).
[28]I. Turek, V. Drchal, J. Kudrnovský, M. Šob, and P. Weinberger, *Electronic Structure of Disordered Alloys, Surfaces and Interfaces* (Kluwer Academic, Boston, 1997).
[29]S. H. Vosko, L. Wilk, and M. Nusair, Can. J. Phys. **58**, 1200 (1980).
[30]U. Sivan and Y. Imry, Phys. Rev. B **33**, 551 (1986).
[31]A. L. Wysocki, R. F. Sabirianov, M. van Schilfgaarde, and K. D. Belashchenko, Phys. Rev. B **80**, 224423 (2009).
[32]J. Kudrnovský, V. Drchal, I. Turek, S. Khmelevskyi, J. K. Glasbrenner, and K. D. Belashchenko, Phys. Rev. B **86**, 144423 (2012).
[33]W. H. Butler, X. G. Zhang, D. M. C. Nicholson, T. C. Schulthess, and J. M. MacLaren, J. Appl. Phys. **79**, 5282 (1996).
[34]K. Xia, M. Zwierzycki, M. Talanana, P. J. Kelly, and G. E. W. Bauer, Phys. Rev. B **73**, 064420 (2006).
[35]J. Binder, P. Zahn, and I. Mertig, J. Appl. Phys. **87**, 5182 (2000).
[36]C. Blaas, L. Szunyogh, P. Weinberger, C. Sommers, P. M. Levy, and J. Shi, Phys. Rev. B **65**, 134427 (2002).
[37]C. Sommers and P. Weinberger, Phys. Rev. B **72**, 054431 (2005).
[38]M. Przybylski, M. Dabrowski, U. Bauer, M. Cinal, and J. Kirschner, J. Appl. Phys. **111**, 07C102 (2012).
[39]M. Czerner, M. Bachmann, and C. Heiliger, Phys. Rev. B **83**, 132405 (2011).
[40]M. Oshita, S. Yotsuhashi, H. Adachi, and H. Akai, J. Phys. Soc. Jpn. **78**, 024708 (2009).